Journal of Power Sources 232 (2013) 297–305

Contents lists available at SciVerse ScienceDirect

Journal of Power Sources

journal homepage: www.elsevier.com/locate/jpowsour

Sorption and transport properties of 2-acrylamido-2-methyl-1-propanesulfonic acid-grafted bacterial cellulose membranes for fuel cell application

C.W. Lin [a,*], S.S. Liang [a], S.W. Chen [a], J.T. Lai [b]

[a] Department of Chemical and Materials Engineering, National Yunlin University of Science and Technology, Douliu, Yunlin 640, Taiwan
[b] Food Industry Research and Development Institute, HsinChu, Taiwan

HIGHLIGHTS

- This work pioneers the exploration of bacterial cellulose-based proton-conducting membranes for DMFCs.
- An effective modification of BC membrane with high conductivity is proposed.
- The modified BC membrane exhibits exceptional methanol-inhibiting behavior.
- The AMPS10-*g*-BC membrane used in DMFC is advantageous to be operated under higher methanol concentration.

ARTICLE INFO

Article history:
Received 23 October 2012
Received in revised form
7 January 2013
Accepted 10 January 2013
Available online 21 January 2013

Keywords:
Bacterial cellulose
2-acrylamido-2-methyl-1-propanesulfonic acid
Proton-conducting membrane
Self-diffusion coefficient
Methanol permeability
Direct methanol fuel cell

ABSTRACT

This study investigated the sorption and transport properties of proton-conducting membranes based on a bacterial cellulose (BC) biopolymer with 2-acrylamido-2-methyl-1-propanesulfonic acid (AMPS) grafted using ultraviolet (UV)-induced polymerization. The transport properties of the membranes were characterized according to their self-diffusion coefficients and methanol permeabilities. Using pulsed field-gradient nuclear magnetic resonance (PFG-NMR) technology, the water and methanol self-diffusion coefficients through the AMPS-*g*-BC membrane were identified as 1.48×10^{-5} cm^2 s^{-1} and 5.30×10^{-6} cm^2 s^{-1}, respectively. The methanol permeability of the AMPS-*g*-BC membrane was 5.64×10^{-7} cm^2 s^{-1}, which was approximately 42% of that of Nafion 115. The differences in the transport behaviors of the Nafion 115 and AMPS-*g*-BC membranes correlated with the sorption characteristics of solvent uptake and lambda (λ) values (number of solvent molecules absorbed per sulfonic acid). The ratio of the water and methanol λ values (i.e., $\lambda_{CH_3OH}/\lambda_{H_2O}$) for the AMPS-*g*-BC membrane was 0.07, which indicated its sorption preference for water compared to methanol. Overall, results indicate that the AMPS-*g*-BC membrane is an effective methanol barrier and a potential solid electrolyte candidate for direct methanol fuel cells.

1. Introduction

Proton-conducting membranes play an important role in fuel cell technology because of their use as separators and proton conductors. Nafion, the current commercially used perfluorosulfonic acid membrane, has a cluster structure with phase separation performed by its hydrophobic fluorocarbon and pendant sulfonic acid groups [1]. Although the Nafion membrane shows good stability and high proton conductivity, some serious drawbacks exclude it from application in direct methanol fuel cells (DMFC). Its major drawback is its unacceptably high methanol permeability, which leads to fuel waste and loss of performance at the cathode because of oxygen consumption and catalyst poisoning [2,3]. Therefore, proton exchange membrane (PEM) materials with low methanol permeability and high proton conductivity are particularly desirable for early commercialization of DMFC.

Recent studies have investigated alternative economic materials with novel hydrocarbon polymers synthesized or combined with a methanol-inhibiting material [4–6]. Investigators have proposed sulfonated aromatic hydrocarbon polymer membranes as low cost alternatives to Nafion. The additional advantages of sulfonated aromatic hydrocarbon membranes are thermal stability and low methanol permeability. However, their proton conductivities are inferior to that of Nafion [7]. Poly(2-acrylamido-2-methyl-1-

* Corresponding author. Tel.: +1 886 5 534 2601x4613; fax: +1 886 5 531 2071.
E-mail address: lincw@yuntech.edu.tw (C.W. Lin).

0378-7753/$ – see front matter © 2013 Elsevier B.V. All rights reserved.
http://dx.doi.org/10.1016/j.jpowsour.2013.01.047

propanesulfonic acid) (PAMPS) displays higher proton conductivity than partially hydrated Nafion because of the sulfonic acid groups in its chemical structure; thus, it forms a component in a novel proton-conducting electrolyte membrane [8,9]. However, because PAMPS is highly water-soluble, a major research objective has been to fix the PAMPS in stable structures while maintaining its high proton conductivity; for example, through the introduction of a copolymer [9,10].

Bacteria produce bacterial cellulose (BC) [11] through the linkage of β-1.4 glycoside to β-D-glucose. Approximately 10 of the linked chains form a microfibril, and then several to >100 of the microfibrils form a fibril. The diameter of BC microfibrils is approximately 20–50 nm. The microfibrils form a three-dimensional reticulum matrix through hydrogen bonding. BC has unique physical properties, including high mechanical stiffness and strength, high moisturizing nature, high crystallinity, broad chemical modifying capacity, and biodegradability [12]. Previous studies have used chemical treatments to improve the electro-mechanical properties of cellulose [13–15].

In principal, a logical method for the development of PEM materials would allow the passage of water but restrict the movement of methanol. The solubility and diffusion properties of the permeating solvent in the membrane, at the given temperature and conditions, determine membrane permeability. The solubility of the solvent in the polymeric membrane is dependent on the chemical nature of the solvent and the corresponding membrane, whereas diffusion is mainly determined by the morphology of the membrane and the properties of the solvent [16]. Sorption data provide a qualitative measure of the solubility of a solvent into a polymer; however, they do not provide information on the diffusion of the solvent into the polymer. Previous studies have described that the water/methanol uptake per Nafion sulfonic acid group is equal in membranes equilibrated in pure water and in pure methanol [17,18]. Huang et al. [18] and Hietala et al. [19] reported that the water and methanol self-diffusion coefficients in the Nafion membrane and in solution display nonsignificant differences.

Although several investigators [20–22] have proposed the potential use of BC as a material source for environmentally compatible ion-exchange membranes for fuel cells, a study on a BC-based proton-conducting membrane for DMFC has yet to be published. This study, therefore, investigated BC-based proton-conducting membranes by modifying bacterial cellulose membranes with 2-acrylamido-2-methyl-1-propanesulfonic acid (AMPS) using ultraviolet (UV)-induced grafting polymerization. It aimed to establish the relationship between the transport and sorption properties of water and methanol in the membranes and their DMFC power performances.

2. Experimental

2.1. Materials

2-acrylamido-2-methyl-1-propanesulfonic acid (AMPS) was purchased from Merck, Germany. The BC membrane was supplied by the Food Industry Research and Development Institute (FIRDI), Taiwan. Benzophenone (BP), isopropanol, acetone, and methanol were purchased from Aldrich, USA.

2.2. Preparation of membranes

Scheme 1 displays the preparation procedures for grafting AMPS monomers onto the BC biopolymer using BP as a photoinitiator. During the radiation procedure, a BC membrane was immersed in BP methanol solution for 3 h. It was then activated using UV light (400 W, 110–400 nm mercury lamp) for 60 s in a nitrogen atmosphere. As shown in Scheme 1(a), during this step, BP abstracted hydrogen atoms from the membrane substrate (BC) to generate surface radicals and semipinacol radicals, which combined to form surface photoinitiators [23]. An AMPS solution (10–20 wt.%) was then added to the reaction chamber and irradiated with UV light for 1 min. As shown in Scheme 1(b), during this step, the introduction of the monomer (AMPS) to the active membrane substrate (BC) initiated the graft polymerization process. The resulting AMPS-*g*-BC membrane was then washed several times with methanol/acetone to remove unreacted homopolymers and monomers.

2.3. Characterization of membranes

2.3.1. Fourier transform infrared spectroscopy

Fourier transform infrared spectroscopy (FT-IR) was performed in a transmittance mode using a spectrophotometer (Spectrum One, Perkin Elmer, USA). Four scans were collected in all spectra at a resolution of 32 cm^{-1}.

2.3.2. Themogravimetric analysis (TGA)

Membrane TGA measurements were collected in a nitrogen atmosphere. The tested samples were 10 mg in weight and the heating rate was 10 °C min^{-1}. Thermograms were obtained in the temperature range 30–700 °C.

2.3.3. Degree of AMPS grafting

The degree of AMPS grafting was evaluated according to changes in membrane weight pre- and postgrafting polymerization using the following equation [24]:

$$DOG = \frac{m_{\text{grafted}} - m_{\text{initial}}}{m_{\text{initial}}} \times 100\% \quad (1)$$

where *DOG* is the degree of grafting (i.e., the ratio of the weight gain), m_{initial} is the initial BC membrane weight, and m_{grafted} is the membrane weight after the grafting process.

2.3.4. Water/methanol solvent uptake

The water/methanol solvent uptakes of the membranes were determined according to differences in the membrane weights pre- and postimmersion in the water/methanol solution overnight. The surface of the membrane sample was wiped with filter paper to remove excess water, after which the wet membrane (W_{wet}) was weighed immediately. The dry membrane (W_{dry}) was weighed after drying at 60 °C for 24 h. The water/methanol solvent uptake (%) was calculated using the following equation:

$$\text{Water/methanol uptake (\%)} = \frac{W_{\text{wet}} - W_{\text{dry}}}{W_{\text{dry}}} \times 100 \quad (2)$$

2.3.5. Ion-exchange capacity and lambda value

A titration method was used to determine the ion-exchange capacity. Each membrane sample was soaked in 50 ml of a 1 M sodium chloride aqueous solution overnight to exchange protons with sodium ions. The ion-exchanged solution was then titrated with a 0.005 M sodium hydroxide solution. The ion-exchange capacity was determined using the following equation:

$$IEC = \frac{M_{\text{i,NaOH}} - M_{\text{f,NaOH}}}{W_{\text{dry}}} = \frac{H^+ \text{ (mmol)}}{W_{\text{dry}}} \quad (3)$$

where $M_{\text{i, NaOH}}$ is the initial mmol of NaOH for titration and $M_{\text{f, NaOH}}$ is the mmol (m_{eq}) of NaOH postequilibrium, H^+ is the molar

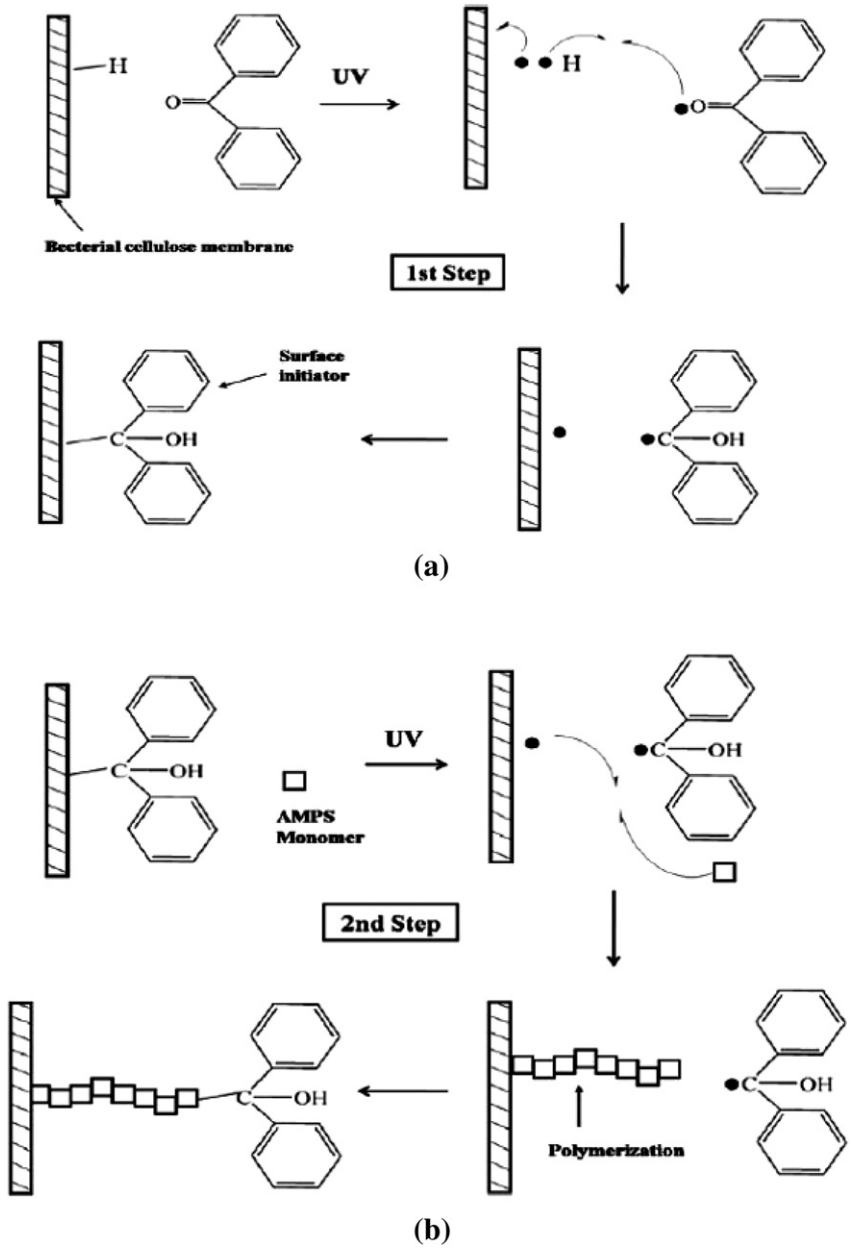

Scheme 1. Schematic diagram of the process for UV-induced grafting polymerization of AMPS monomers onto the BC membrane.

number of proton sites in the membrane, and W_{dry} is the dry membrane weight (g).

The lambda (λ) value, which represents the number of water molecules surrounding an acid site in a membrane, was calculated from the water uptake and *IEC* values using

$$\lambda_{H_2O} = \frac{\left(W_{wet} - W_{dry}\right)/MW_{H_2O}}{IEC \times W_{dry}} \times 1000 = \frac{n(H_2O)}{n(\text{acid groups})} \quad (4)$$

where MW_{H_2O} is the molecular weight of water (18.01 g mol^{-1}) and *IEC* is the ion-exchange capacity (mmol g^{-1}) of the membrane.

2.3.6. Membrane water and methanol self-diffusion coefficients

Membranes were soaked in water or methanol solution for at least 24 h before testing. After removing the surface solvent, the AMPS-*g*-BC membrane was immediately placed in a nuclear magnetic resonance (NMR) tube and sealed. The self-diffusion coefficient was determined using a Varian Infinity Plus-500 NMR spectrometer (Varian, Inc., Palo Alto, CA). The pulsed gradient spin-echo (PGSE) pulse sequence was initiated using a 90° pulse and followed by two identical gradient pulses, separated by a 180° pulse. Experiments were performed with decreasing pulse strength; ranging from 250 G cm^{-1} to 25 G cm^{-1}. The signal intensity (A), as a function of gradient strength (g), was recorded. The expected dependence of signal attenuation on gradient strength [25] is

$$\ln \frac{A(2\tau)}{A_0(2\tau)} = -\left[(\gamma_H G\delta)^2 \left\langle \Delta - \frac{\delta}{3} \right\rangle\right] D \quad (5)$$

where $A(g)$ is the signal intensity as a function of the applied gradient g, $A(0)$ is the signal intensity obtained in the absence of an applied gradient, D is the diffusion coefficient, γ is the nuclear

gyromagnetic ratio, Δ is the time for diffusion between gradient pulses, and δ is the length of the gradient pulse.

2.3.7. Proton conductivity and methanol permeability

Proton conductivity measurements were performed at an ambient temperature after equilibrating the membrane in deionized water for 24 h. Conductivities of fully hydrated membranes were measured using a two-electrode configuration. The conductivity cell contained two stainless steel electrodes with a diameter of 9.45 mm. The membrane sample was sandwiched between these two flat circular electrodes. AC impedance spectra of the membranes were recorded from 70,000 Hz to 100 Hz with an amplitude of 5 mV using an Autolab PGSTST30 instrument. The resistance value associated with the membrane conductivity was determined from the high-frequency intercept of the impedance with the real axis. The conductivity was calculated using

$$\sigma = \frac{L}{RA} \tag{6}$$

where σ, L, R, and A represent the membrane conductivity, membrane thickness, the measured resistance on the membrane, and the cross-sectional area of the membrane perpendicular to the current flow, respectively.

The methanol permeability of membranes was determined using a home-made side-by-side glass diffusion cell. This cell consisted of two compartments of approximately 80 ml, separated by a test membrane with a cross-sectional area of 3.19 cm^2. The membranes were placed between the two compartments using a screw clamp. Prior to all experiments, the membranes were equilibrated in water for 1 d. The receptor compartment was filled with water, whereas the donor compartment was filled with a 3 wt.% methanol solution. The concentration of methanol in the receptor compartment was measured using gas chromatography (China Chromatography 9800) at regular intervals. Methanol permeability was determined from the slope of the plot of methanol concentration in the receptor compartment versus time as described previously [26].

2.3.8. Fabrication of membrane electrode assemblies (MEA) and evaluation of single cell performance

For single cell performance tests of H_2/O_2 FC and DMFC, MEA were fabricated using Nafion 115 and AMPS10-*g*-BC membranes. For H_2/O_2 fuel cell tests, E-TEK electrodes with 0.4 mg cm^{-2} platinum (Pt) loading and 0.6 mg cm^{-2} impregnated Nafion were used. The electrodes were placed on both sides of the membrane with no special treatment, such as hot-pressing, provided to optimize the electrode/membrane interface. The MEA was assembled in the test cell and its performance was evaluated using pure hydrogen as fuel and oxygen as an oxidant. Home-made electrodes were used to fabricate the MEA for the DMFC using a hot-pressing method at 110 °C for 90 s under a pressure of 100 atm. The cathode consisted of a Teflonized carbon cloth support, upon which a thin layer of uncatalyzed carbon, bound with polytetrafluoroethene (PTFE), was coated homogeneously. Carbon-supported Pt bound with Nafion was coated as a catalyst layer onto this diffusion layer to provide a metal loading of 3 mg cm^{-2}. The anode was constructed using the same method except the binder in the diffusion layer was Nafion instead of PTFE. Carbon-supported platinum–ruthenium (Pt–Ru) was used as an anode catalyst for DMFC. A thin layer of Nafion solution (0.6 mg cm^{-2} loading) was spread onto each electrode and dried in an oven at 80 °C for 2 h before hot-pressing. The polarization measurements were performed using a MACCOR Model 2200 fuel cell test station. The gases were allowed to pass through stainless steel humidifiers before entering the fuel cell inlets and the flow rates were controlled by mass flow controllers. Methanol solution was fed using a small pump (FMI 'Q' pump) with a flow rate of 3 ml min^{-1}.

Table 1
Degree of AMPS grafting of BC membranes obtained from different AMPS concentrations.

AMPS concentration (%)	Membrane	Degree of grafting (%)
10	AMPS10-*g*-BC	5.61 ± 0.57
15	AMPS15-*g*-BC	28.6 ± 0.11
20	AMPS20-*g*-BC	39.51 ± 0.12

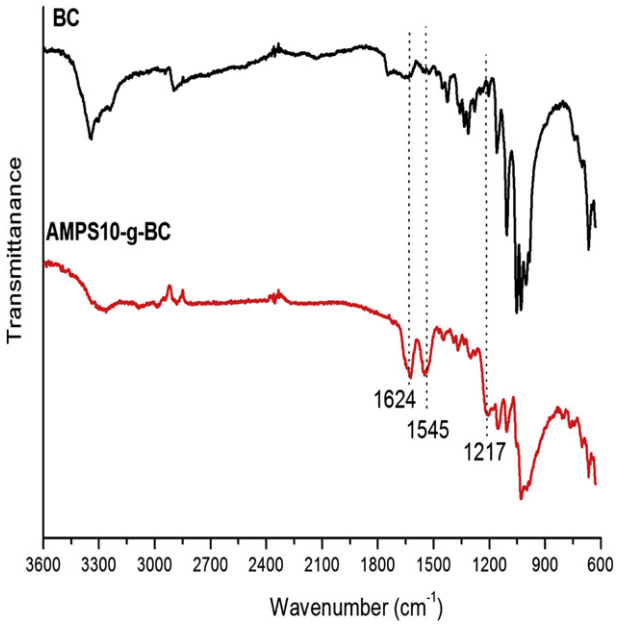

Fig. 1. FT-IR spectra of pristine BC and AMPS10-*g*-BC membranes.

3. Results and discussion

3.1. Characterization of AMPS-g-BC membranes

Table 1 shows the degree of AMPS grafting onto the BC membranes using different AMPS solutions. Increasing AMPS

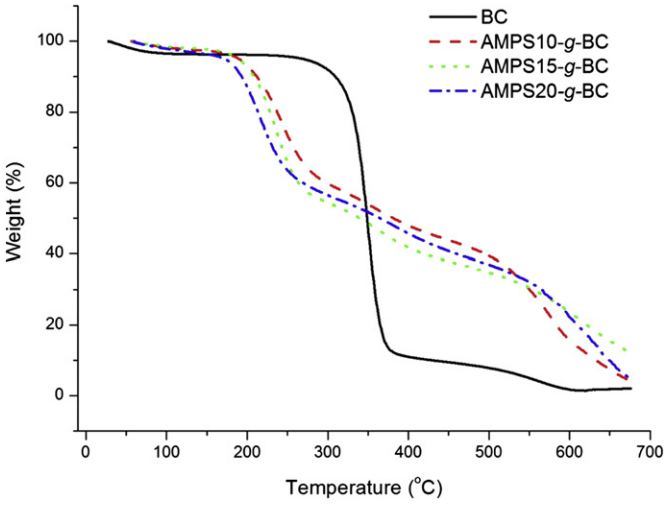

Fig. 2. TGA curves of pristine BC and AMPS10-*g*-BC membranes.

concentration led to increased AMPS grafting level, up to a maximum *DOG* value of 39.5% when the AMPS concentration was 20% (i.e., AMPS20-*g*-BC). This result indicated that higher AMPS concentration promotes the grafting of sulfonic acid onto BC membranes.

Fig. 1 compares the FT-IR spectra of the BC membranes pre- and post-AMPS grafting. The pristine BC membrane shows a characteristic hydroxyl group absorption band at 3200–3400 cm^{-1}. However, following the grafting of AMPS, characteristic bands at 1624 cm^{-1} and 1545 cm^{-1}, corresponding to the C=O and NH group on AMPS, respectively, were observed [27]. A sharp band at 1217 cm^{-1}, reflecting the sulfonic acid group on AMPS, was also obtained. These results indicated the successful UV-induced grafting of AMPS onto the BC membranes.

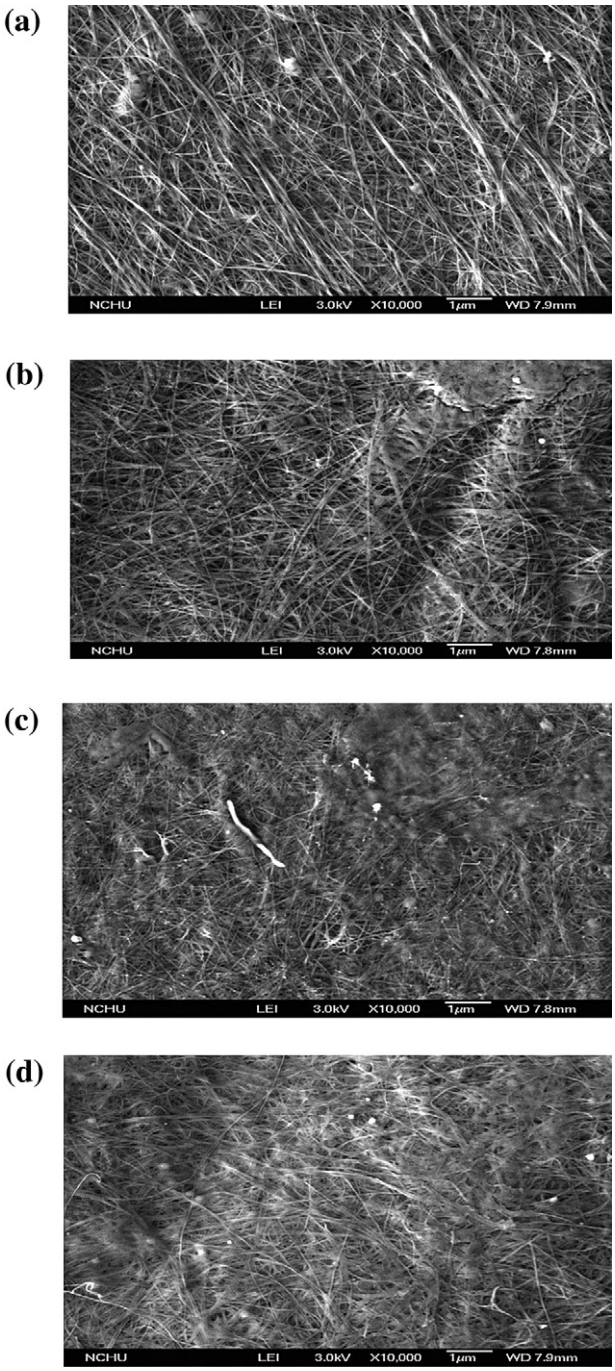

Fig. 3. Scanning electron micrographs of the surface of BC and AMPS-*g*-BC membranes: (a) pristine BC, (b) AMPS10-*g*-BC, (c) AMPS15-*g*-BC, (d) AMPS20-*g*-BC.

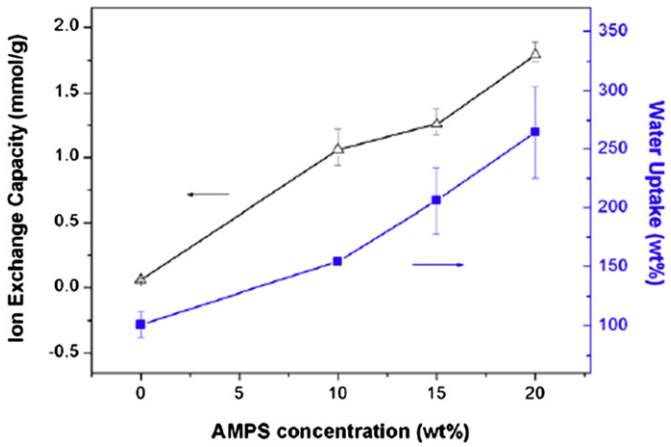

Fig. 4. Effects of AMPS concentration on the water uptake and *IEC* values of various AMPS-*g*-BC membranes.

The thermal degradation curves of the membranes obtained pre- and post-AMPS grafting were used to further identify the grafting of AMPS onto the BC membranes (Fig. 2). The pristine BC membrane showed two major weight loss stages at 350 °C and 550 °C. The first, at 350 °C, could be attributed to concurrent cellulose degradation processes such as depolymerization, dehydration, and decomposition of glycosyl units followed by the formation of a charred residue. The second, at approximately 550 °C, was related to the oxidation and/or breakdown of the charred residue to lower molecular weight gaseous products [28]. The AMPS10-*g*-BC membrane exhibited three weight loss stages at 216–243 °C, 358–376 °C, and 573–620 °C. The weight loss in the first, second, and third stages could be attributed to the decomposition of sulfonic acid groups, cellulose degradation, and the breakdown of the charred residue, respectively [27,28]. These results further confirmed successful AMPS grafting onto the BC membrane and indicate an efficient method for AMPS grafting onto BC membranes.

Fig. 3 displays typical surface morphologies of the pristine BC membrane and AMPS10-*g*-BC, AMPS15-*g*-BC, and AMPS20-*g*-BC

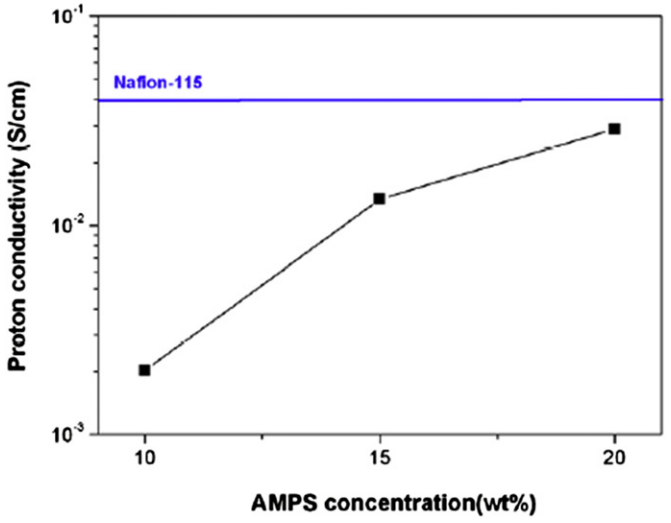

Fig. 5. Effects of AMPS concentration on the proton conductivities of AMPS-*g*-BC membranes.

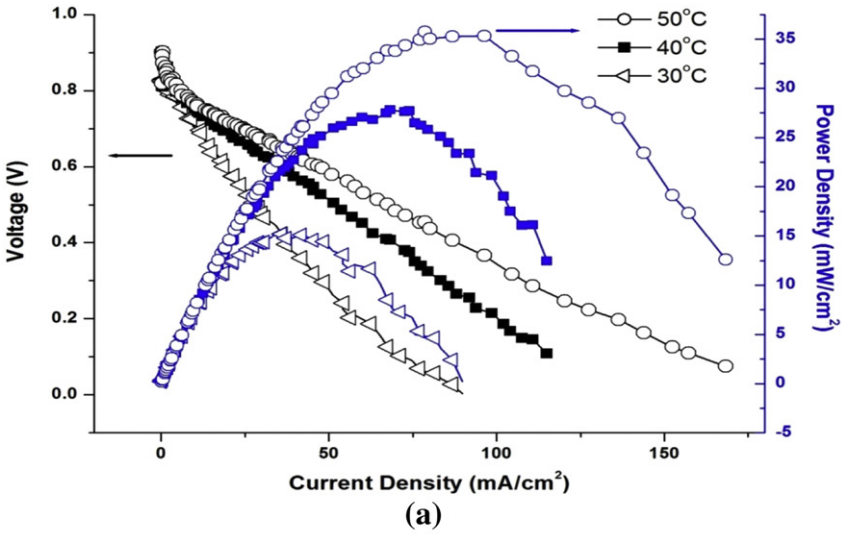

Fig. 6. Polarization curves of MEA containing AMPS-*g*-BC membranes at different temperatures using H_2 and O_2 as reactants: (a) AMPS10-*g*-BC, (b) AMPS15-*g*-BC, (c) AMPS20-*g*-BC.

membranes. The scanning electron micrograph (SEM) image in Fig. 3(a) shows a side view of the BC nanofiber membrane, with an average diameter of approximately 42 nm and a length ranging from a few micrometers to >100 μm. As shown in Fig. 3(a), the BC membrane contains interconnecting pores ranging in size from 10 μm to 15 μm. As shown in Fig. 3(c) and (d), the AMPS-*g*-BC membranes showed increased structure density with increasing *DOG*. In the SEM images, at a lower AMPS grafting level, membranes showed a more expanded structure with pores. At a higher *DOG*, however, the membrane surface was dense with decreased pore distribution.

3.2. Basic properties of the AMPS-g-BC membranes: water uptake, IEC, proton conductivity

Fig. 4 displays the water uptake and *IEC* values of the AMPS-*g*-BC membranes. The *IEC* values and water uptake both increased with increasing AMPS concentration. The *IEC* values of the membranes increased from 0.09 g^{-1} to 1.79 mmol g^{-1} when the AMPS concentration increased from 0% to 20%. This increasing *IEC* value corresponded with the increased amount of sulfonic acid on AMPS-*g*-BC membranes modified with higher AMPS concentration. Increased sulfonic acid also led to increased water uptake into the AMPS-*g*-BC membranes. When AMPS concentration increased from 0% to 20%, the water uptake of the AMPS-*g*-BC membranes increased from 100% to 264%. Increased sulfonic acid on the AMPS-*g*-BC membranes at higher AMPS concentrations can explain this trend. Higher AMPS concentration also induced a higher degree of AMPS grafting and sulfonic acid on the BC membrane, and contributed to higher *IEC* values and water uptake.

Fig. 5 displays the proton conductivity of the AMPS-*g*-BC membranes as a function of AMPS concentration at room temperature. The proton conductivity of the AMPS-*g*-BC membranes increased with increasing AMPS grafting level to a maximal value of 2.9×10^{-2} S cm^{-1} in the AMPS20-*g*-BC membrane. This increased proton conductivity was in accordance with the *IEC* and water uptake values, which both promote the transportation of protons in membranes. Specifically, this proton conductivity value is close to that of Nafion 115 measured under the same experimental conditions. In this study, Nafion 115 proton conductivity was 3.9×10^{-2} S cm^{-1}, which correlated with values reported previously [29,30]. These similar proton conductivities demonstrated

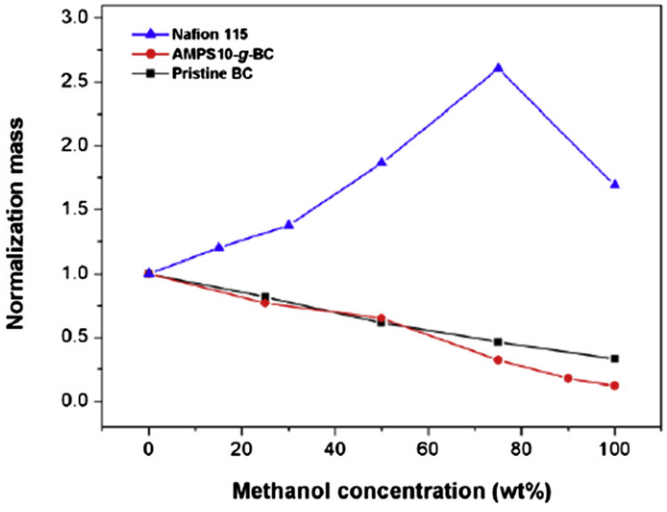

Fig. 7. Normalized solvent uptakes of pristine BC, AMPS10-*g*-BC and Nafion 115 membranes at different methanol concentrations.

Table 2
Lambda values of water and methanol in AMPS10-*g*-BC and Nafion 115 membranes.

Membrane	*IEC* (mmol g^{-1})	Water uptake (%)	Methanol uptake (%)	λ_{H_2O}	λ_{CH_3OH}	$\lambda_{CH_3OH}/\lambda_{H_2O}$
Nafion® 115	0.99	28.5	60.0	16.5	19.6	1.19
AMPS10-*g*-BC	1.06	154.1	18.7	80.8	5.5	0.07

the potential of the AMPS-*g*-BC membranes for fuel cell application. To further evaluate the feasibility of the AMPS-*g*-BC membranes for use in fuel cells, a polarization curve of the single cell assembled with the AMPS-*g*-BC membrane was determined.

3.3. Polarization characteristics of the MEA containing AMPS-g-BC membranes

Fig. 6(a)–(c) displays the polarization characteristics of the MEA containing AMPS10-*g*-BC, AMPS10-*g*-BC, and AMPS20-*g*-BC membranes at different reaction temperatures. The fuel cell performances of the AMPS-*g*-BC membranes increased with increasing cell temperature. For example, in the AMPS20-*g*-BC membrane, the power density increased from 61 mW cm^{-2} to 97 mW cm^{-2} when cell temperature increased from 30 °C to 50 °C. Similar trends were observed in the AMPS10-*g*-BC and AMPS15-*g*-BC membranes. The AMPS20-*g*-BC membrane showed significantly superior power density to the AMPS10-*g*-BC and AMPS15-*g*-BC membranes, which correlated with its higher proton conductivity. These results indicated that the grafting of AMPS onto BC provides a promising method for the preparation of proton exchange membranes for fuel cell application using hydrogen/oxygen as a reactant. This study further investigated the feasibility of AMPS-*g*-BC membranes for DMFC application.

It should be noted that the AMPS-*g*-BC membranes exhibit an unacceptable water uptake of more than 200% at an AMPS concentration of 15%. This excessive water uptake could lead to loss of mechanical stability of the polymeric membrane because the excessive water might cause high stress on the local bonds of the membrane and interrupt the integration of the membrane structure [31]. This problem might increase in severity when using liquid methanol solution instead of hydrogen gas as a reactant. To reduce this problem, this study therefore selected the AMPS10-*g*-BC membrane with a relatively lower water uptake (154%) to further evaluate the relative water/methanol sorption and transport properties in the AMPS-*g*-BC membrane and demonstrate its feasibility for use in DMFC.

3.4. Water and methanol sorption and transportation properties in the AMPS10-g-BC membranes

3.4.1. Sorption properties of the AMPS10-g-BC membrane

Fig. 7 displays the water/methanol solvent uptake values of the Nafion 115 and AMPS10-*g*-BC membranes as a function of methanol concentration. The Nafion 115 and AMPS10-*g*-BC membranes

Table 3
Water and methanol self-diffusion coefficients of pristine BC, AMPS10-*g*-BC, and Nafion 115 membranes.

Membrane	D_{H_2O} (cm^2 s^{-1})	D_{CH_3OH} (cm^2 s^{-1})	D_{CH_3OH}/D_{H_2O}
Water[a]	2.3×10^{-5}	N/A	N/A
Methanol[a]	N/A	2.4×10^{-5}	N/A
Pristine BC	N/A	4.76×10^{-6}	N/A
AMPS10-*g*-BC	1.48×10^{-5}	5.30×10^{-6}	0.358
Nafion® 115	8.89×10^{-6}	8.63×10^{-6}	1.125

[a] Data obtained from ref. [19].

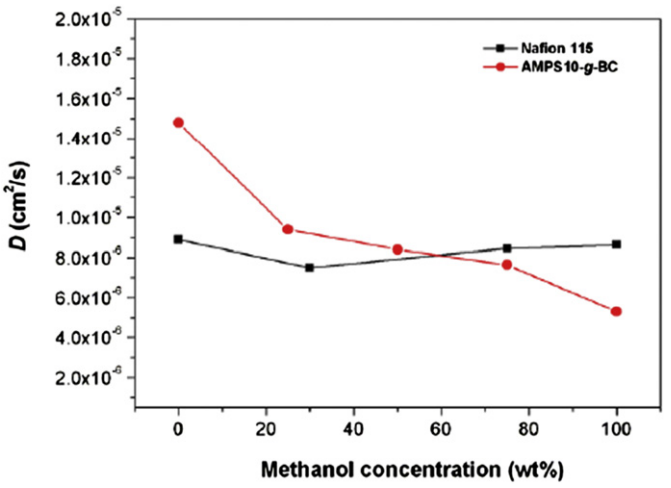

Fig. 8. Water and methanol self-diffusion coefficients of Nafion 115 and AMPS10-*g*-BC membranes at different methanol concentrations.

showed distinctive water/methanol solvent uptake characteristics. The solvent uptake of the AMPS10-*g*-BC membrane reduced from 154.1% to 18.7% with increasing methanol concentration, whereas the solvent uptake of Nafion 115 showed a close to linear increase to a maximal value at a methanol concentration of 75%. These results indicated that the AMPS10-*g*-BC membrane displays excellent resistance to methanol sorption under higher methanol concentrations.

Table 2 shows the λ values of water and methanol in the Nafion 115 and AMPS10-*g*-BC membranes. In Nafion 115, the λ values of water and methanol were similar (16.50 for water and 19.57 for methanol), indicating equal sorption preference for water and methanol. This finding supported those reported previously [17,30]. The Nafion membrane's similar preferences for water and methanol might contribute to higher water/methanol solvent uptake at high methanol concentrations. Ren et al. [17] reported that methanol and water both permeate the Nafion membrane. At low methanol concentrations, this process increases with increasing methanol concentration. At high methanol concentrations, however, water starts to become excluded. In the AMPS10-*g*-BC membrane, the λ-value of methanol differs greatly from that of water. As shown in Table 2, in the AMPS10-*g*-BC membrane, the methanol λ-value is 5.5, which is approximately 7% of that of water (80.8). This result indicated that the AMPS10-*g*-BC membrane has higher sorption preference for water than methanol and that this preference might contribute to decreased solvent uptake at higher methanol concentrations (Fig. 7).

Table 4
Comparisons of lambda value, self-diffusion coefficient, and methanol permeability of AMPS10-*g*-BC and Nafion 115 membranes.

Membrane	$\lambda_{CH_3OH}/\lambda_{H_2O}$	D_{CH_3OH}/D_{H_2O}	Methanol permeability ($cm^2\ s^{-1}$)
AMPS10-g-BC	0.07	0.358	5.64×10^{-7}
Nafion 115	1.19	1.125	1.33×10^{-6}

Previous studies have reported that a membrane's preference for sorption of water or methanol usually correlates with its transport properties [18,32]. Therefore, this study included the evaluation of the relative transport properties of water and methanol in membranes, such as the water and methanol self-diffusion coefficients and methanol permeability, to further identify their transport behaviors in the AMPS10-*g*-BC membrane.

3.4.2. Self-diffusion coefficients

Self-diffusion coefficient analysis precedes the measurement of methanol permeability and indicates the transport of water and methanol molecules through a membrane cross-section. Table 3 displays the water and methanol self-diffusion coefficients in the AMPS10-*g*-BC and Nafion 115 membranes. In Nafion 115, the water self-diffusion coefficient was $8.89 \times 10^{-6}\ cm^2\ s^{-1}$, which supported the findings of previous studies [17,19]. The methanol self-diffusion coefficient in Nafion 115 was $8.63 \times 10^{-6}\ cm^2\ s^{-1}$, which was similar to its water self-diffusion coefficient. This result indicated that the Nafion 115 membrane displays no selectivity for the transport of water or methanol and is consistent with the water/methanol sorption results shown in Fig. 7. In the AMPS10-*g*-BC membrane, however, methanol self-diffusion showed marked differences from that of water. Its methanol self-diffusion coefficient of

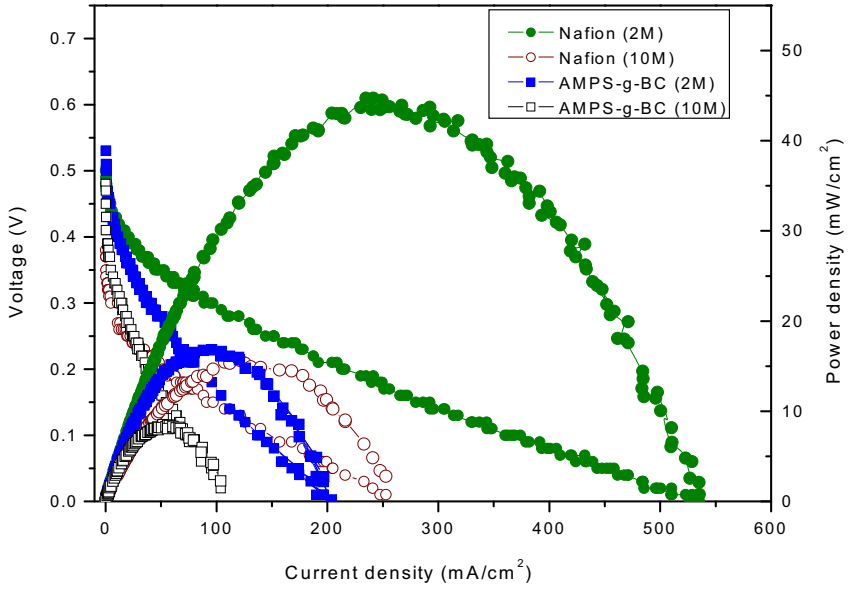

Fig. 9. Polarization curves and power densities of DMFC using the AMPS10-*g*-BC membrane at different methanol concentrations.

5.3×10^{-6} cm^2 s^{-1} was lower than that of water (1.48×10^{-5} cm^2 s^{-1}). Table 3 also displays the self-diffusion coefficient ratio of water to methanol in the membranes, expressed as D_{CH_3OH}/D_{H_2O}. The self-diffusion coefficient ratio of the AMPS10-*g*-BC membrane was 0.358, which was approximately one-third of that of Nafion 115 (1.125). This result indicated that the AMPS10-*g*-BC membrane has higher selectivity for the transport of water than methanol and correlated with its water and methanol λ values.

To further identify the water/methanol transport properties in the AMPS10-*g*-BC and Nafion 115 membranes, the water/methanol self-diffusion coefficients in the membranes were measured at different methanol concentrations and compared. As shown in Fig. 8, the water/methanol self-diffusion coefficients in the Nafion 115 membrane increased with increasing methanol concentration, whereas those of the AMPS10-*g*-BC membrane showed a decreasing trend with increasing methanol concentration. This result further indicated that the AMPS10-*g*-BC membrane displays methanol-inhibiting characteristics.

3.4.3. Methanol permeability

Table 4 presents the methanol permeabilities of the AMPS10-*g*-BC membranes as a function of methanol concentration. In this study, the methanol permeability of Nafion 115 was 1.33×10^{-6} cm^2 s^{-1}, which supported previous findings [33]. The methanol permeability of the AMPS10-*g*-BC membrane was 5.64×10^{-7} cm^2 s^{-1}; approximately 50% of that of Nafion 115. These results correlated with the previously described trends in water/methanol sorption and diffusion coefficients in the AMPS10-*g*-BC and Nafion 115 membranes.

3.4.4. DMFC performances

Fig. 9 compares the DMFC performances of the MEA using Nafion 115 and AMPS10-*g*-BC membranes, respectively. The power density using a 2 M methanol solution was 16 mW cm^{-2}, which was approximately 35% of that of Nafion 115. The power density using 10 M methanol solution was approximately 9 mW cm^{-2}, which was approximately 60% of that of Nafion 115. It is, therefore, relatively advantageous for the AMPS10-*g*-BC membrane to be used in higher methanol concentrations. The open-circuit voltage (OCV) for the modified BC-based fuel cell was higher than that for the Nafion-based one. The group is currently making effective approaches to reduce excessive swelling of the AMPS-*g*-BC membrane for its effective implementation in DMFC.

4. Conclusions

This study investigated the modification of BC membranes using AMPS as a grafting agent and a UV-induced graft polymerization technique. Results indicate that it is possible to graft AMPS to the BC membrane, retain its proton conductivity, and yield favorable fuel cell performance. In the AMPS10-*g*-BC membrane, the ratio of self-diffusion coefficients of methanol to water (i.e., D_{CH_3OH}/D_{H_2O}) is 0.358. The methanol permeability of the AMPS10-*g*-BC membrane is 5.64×10^{-7} cm^2 s^{-1}, which is approximately 42% of that of Nafion 115. The solvent uptake of the AMPS10-*g*-BC membrane decreases gradually with increasing methanol concentration. In the AMPS10-*g*-BC membrane, the ratio of methanol and water λ values (i.e., $\lambda_{CH_3OH}/\lambda_{H_2O}$) is 0.07, which indicates sorption preference for water compared to methanol. Overall, these results indicate that the AMPS10-*g*-BC membrane is an effective methanol barrier and a potential candidate for use in DMFC.

Acknowledgement

Financial support from the National Science Council (under contract numbers 99-ET-E-224-002-ET) is gratefully acknowledged. The authors are grateful to Mr. J. C. Ho from the Food Industry Research and Development Institute (FIRDI) for preparing and providing bacteria cellulose membranes.

References

[1] T.D. Gierke, G.E. Munn, F.C. Wilson, J. Polym. Sci. Polym. Phys. Ed. 19 (1981) 1687–1704.
[2] X. Ren, P. Zelency, S. Thomas, J. Davey, S. Gottesfeld, J. Power Sources 86 (2000) 111–116.
[3] K. Lee, J.D. Nam, J. Power Sources 157 (2006) 201–206.
[4] L. Li, J. Zhang, Y. Wang, J. Membr. Sci. 226 (2003) 159–167.
[5] F. Wang, M. Hicker, Y.S. Kim, T.A. Zawodzinski, J.E. McGrath, J. Membr. Sci. 197 (2002) 231–242.
[6] N. Carretta, V. Tricoli, J. Membr. Sci. 166 (2000) 189–197.
[7] I.M. Krivobokov, E.N. Gribov, A.G. Okunev, Electrochim. Acta 56 (2011) 2420–2427.
[8] J.P. Randin, J. Electrochem. Soc. 129 (1982) 1215–1220.
[9] W. Charles Walker Jr., J. Power Sources 110 (2002) 144–151.
[10] L.E. Karlsson, P. Jannasch, B. Wesslén, Macromol. Chem. Phys. 203 (2002) 686–694.
[11] R. Jonas, F.F. Luiz, Polym. Degrad. Stabil. 59 (1998) 101–106.
[12] D. Klemm, B. Heublein, H.P. Fink, A. Bohn, Angew. Chem. Int. Ed. 44 (2005) 3358–3393.
[13] S. Ifuku, M. Tsuji, M. Morimoto, H. Saimoto, H. Yano, Biomacromolecules 10 (2009) 2714–2717.
[14] A.M.A. Nada, S. Abd El-Mongy, E.S. Abd El-Sayed, BioResources 4 (2009) 80–93.
[15] J. George, K.V. Ramana, S.N. Sabapathy, A.S. Bawa, World J. Microbiol. Biotechnol. 21 (2005) 1323–1327.
[16] K.D. Kreuer, T. Dippel, J. Maier, Proc. Electrochem. Soc. 95 (1995) 241.
[17] X. Ren, T.E. Springer, T.A. Zawodzinski, S. Gottesfeld, J. Electrochem. Soc. 147 (2000) 466–474.
[18] Y.F. Huang, B.J. Hwang, C.W. Lin, J. Appl. Polym. Sci. 113 (2009) 342–350.
[19] S. Hietala, S.L. Maunu, F. Sundholm, J. Polym. Sci. Polym. Phys. Ed. 38 (2000) 3277–3284.
[20] Y.J. Choi, Y. Ahn, M.S. Kang, H.K. Jun, I.S. Kim, S.H. Moon, J. Chem. Technol. Biotechnol. 79 (2004) 79–84.
[21] B.R. Evans, H.M. O'Neill, V.P. Malyvanh, I. Lee, J. Woodward, Biosens. Bioelectron. 18 (2003) 917–923.
[22] J. Yang, D. Sun, J. Li, X. Yang, J. Yu, Q. Hao, W. Liu, J. Liu, Z. Zou, J. Gu, Electrochim. Acta 54 (2009) 6300–6305.
[23] H. Ma, R.H. Davis, C.N. Bowman, Macromolecules 33 (2000) 331–335.
[24] Y. Choi, Y. Ahn, M. Kang, H. Jun, I. Kim, S. Moon, Chem. Technol. Biotechnol. 79 (2004) 79–84.
[25] E.O. Stejskal, J.E. Tanner, J. Chem. Phys. 43 (1965) 3597–3603.
[26] H.Y. Chang, C.W. Lin, J. Membr. Sci. 218 (2003) 295–306.
[27] J. Qiao, T. Hamaya, T. Okada, Polymer 46 (2005) 10809–10816.
[28] M. Roman, W.T. Winter, Biomacromolecules 5 (2004) 1671–1677.
[29] M.A. Hickner, C.H. Fujimoto, C.J. Cornelius, Polymer 47 (2006) 4238–4244.
[30] E. Skou, P. Kauranen, J. Hentschel, Solid State Ionics 97 (1997) 333–337.
[31] H.Strathmann, Membr. Sci. Technol. Ser. 9, (Chapter 3), p. 118.
[32] Y.F. Huang, L.C. Chuang, A.M. Kannan, C.W. Lin, J. Power Sources 186 (2009) 22–28.
[33] Y.F. Huang, A.M. Kannan, C.S. Chang, C.W. Lin, Int. J. Hydrogen Energy 36 (2011) 2213–2220.